Magnesium Technology 2012
Edited by: Suveen N. Mathaudhu, Wim H. Sillekens, Neale R. Neelameggham, and Norbert Hort
TMS (The Minerals, Metals & Materials Society), 2012

SOLID SOLUTION HARDENING EFFECT OF ALUMINUM ON THE CREEP DEFORMATON OF AZ91 MAGNESIUM ALLOY

Farhoud Kabirian[1], Reza Mahmudi[2]

1) Department of Mechanical Engineering, University of Maryland, Baltimore County, USA
2) School of Metallurgical and Materials Engineering, University of Tehran, Tehran, Iran

Keywords: AZ91, Creep Resistance, Solid Solution Hardeing

Abstract

It has been previously shown that separate additions of 2% rare earth elements (RE) and 0.6% Zr to the AZ91 base alloy improve creep properties. However, in this investigation using impression creep method, it is shown that simultaneous addition of these elements not only cannot improve creep properties but also leads to its deterioration. According to the creep deformation mechanism of the base alloy and microstructural evidences, it is believed that this drop in creep resistance mainly stems from depletion of grain interiors and the areas adjacent to grain boundaries from aluminum solute atoms. Reduction of aluminum content as solute atoms is due to the great affinity of RE and Zr atoms for aluminum. This leads to the weakening of Al solute atoms role as obstacles against dislocation movement, even though the volume fraction of the thermally stable particles tends to be high.

Introduction

In recent years, concurrent with the rise of energy issues the transportation industries have paid a great attention to employ light weight materials. Mg-Al-based alloys are most promising for more development. These alloys possess a reasonable combination of enhanced mechanical properties [1–3], good corrosion resistance [4,5], and excellent castability [6]. Despite these advantages, the main problem involved in using Mg-Al alloys is the drastic drop in their high temperature mechanical properties and creep resistance with increasing temperature to above 400 K [7]. Generally, the low creep resistance of Mg-Al alloys, with aluminum contents greater than 3 wt.%, is attributed to the formation of β-Mg17Al12 precipitates at grain boundaries and inter-dendritic regions [1–3]. Due to their low melting point, these precipitates are thermally unstable and thus they can accelerate grain boundary diffusion, resulting in considerable instability of the microstructure in regions adjacent to grain boundaries [3,4].

The AZ91 alloy containing 9 wt.% Al and 1 wt.% Zn is the most commonly used cast magnesium alloy for low-temperature applications. The high percentage of Al in this alloy makes it more susceptible to microstructural instability. Most of the attempts for improving the high-temperature structural stability of this alloy have concentrated on suppressing discontinuous precipitation of β-Mg17Al12 and creating more thermally stable intermetallics in the magnesium matrix. Due to the high affinity of aluminum atoms for elements such as Ca, Ti, Zr, and rare earth (RE), it is possible to reduce the amount of the $Mg_{17}Al_{12}$ by consuming the aluminum content of the alloy to form Al-containing intermetallic compounds with relatively high melting points [8].

Kabirian and Mahmudi [9] have reported that AZ91-2RE, owing to the fine distribution of Al11RE3 intermetallic with branch type morphology, shows the best creep properties among RE containing AZ91 alloys with 1, 2 and 3 wt% RE. In another work, they showed that AZ91-0.6Zr advantaging from favorable combination of solid solution hardening and fine distribution of the thermally stable Al2Zr and Al3Zr2, particles has the superior creep resistance compared to the AZ91-0.2Zr and AZ91-1.0Zr alloys [10,11]. Based on these findings, the aim of the present work is to investigate the influence of simultaneous additions of 0.6 wt% Zr and 2 wt% RE on the microstructure of the AZ91 alloy and its creep resistance via impression creep testing.

Experimental Procedure

The materials used were AZ91 alloy with an actual chemical composition of Mg-8.9 wt.% Al-0.78 wt. %Zn-0.32 wt.% Mn, and the same material with separate and simultaneous additions of 2.0 wt.% RE and 0.6 wt.% Zr. Melting was carried out in an electrical furnace under the Foseco MAGREX 36 covering flux to protect molten magnesium from oxidation. The cast bars were cut into 4-mm slices and tested in an impression tester. The details of the testing arrangement is explained elsewhere [12] and will only be briefly described here. An MTS universal tensile testing machine equipped with a three-zone split furnace was used to perform constant-load impression tests. Impression tests were run at two different temperatures of 425 and 455 K at different stress levels. The cast samples were studied by scanning electron microscopy (SEM) to examine the as-cast microstructure as well as to identify the phases present in the microstructure. X-ray diffraction (XRD) analysis was carried out on selected specimens to identify the existing phases.

Results and Discussion

Figures 1a through 1d show the SEM micrographs of the tested alloys. It can be observed that the microstructure of AZ91 is basically composed of the network-shape eutectic β-$Mg_{17}Al_{12}$ distributed in the magnesium matrix, the volume fraction of which decreases in the other alloys containing Zr and/or RE elements. This can be attributed to the fact that RE elements and Zr consume some of the aluminum to form Al-RE and Al-Zr intermetallic compounds, respectively, leaving less aluminum to combine with the Mg matrix to form β-$Mg_{17}Al_{12}$. Some fine Al-Zr

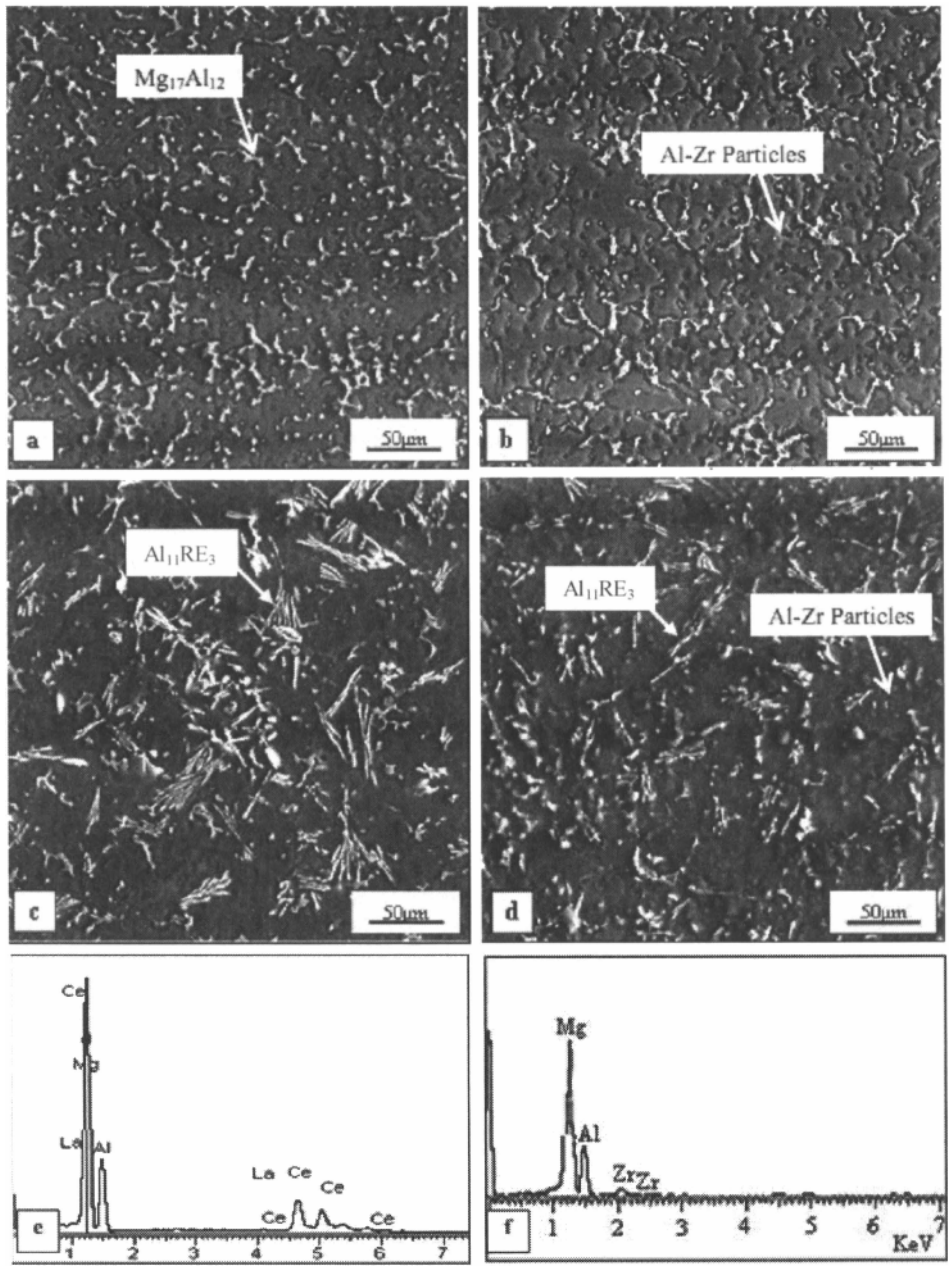

Fig. 1. SEM micrographs of (a) AZ91, (b) AZ91-0.6Zr, (c) AZ91-2RE, (d) AZ91-2RE-0.6Zr alloys. the EDX analysis of (e) acicular and (f) spherical intermetallics.

spherical particles with an average size of about 2 μm have appeared in the microstructure of the AZ91-0.6Zr alloy (Fig. 1b), while needle-shape $Al_{11}RE_3$ particles are dispersed throughout the microstructure of AZ91-2RE, as shown in Fig. 1c. It is worth mentioning that both types of particles have also been detected in the microstructure of AZ91-2RE-0.6Zr in Fig. 1d. The qualitative analysis of acicular and spherical particles determined by the EDS analysis, are shown in Figs. 1e and 1f, respectively. It is evident that La, Ce, and Al are the main constituents of acicular particles (Fig. 1e), while Al and Zr atoms constitute spherical particles (Fig. 1f). To identify the phases present in the tested alloys, XRD spectra were obtained and are shown in Fig. 2. As can be seen, α Mg and β-$Mg_{17}Al_{12}$ are the only phases in the AZ91 alloy, whereas in the AZ91-2RE-0.6Zr alloy, additional peaks are evident. These new peaks correspond to the Al11RE3, Al2Zr, and Al_3Zr_2 intermetallics.

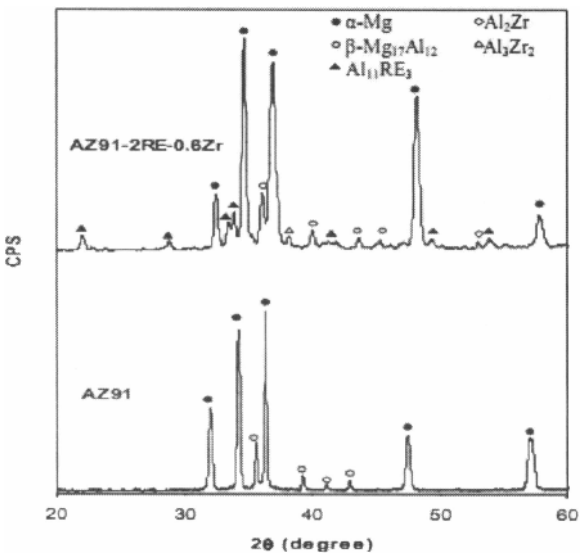

Figure 2. XRD patterns of the tested materials.

Typical impression creep data, presented as the variation of punch penetration depth with dwell time under different stress levels for all materials tested at 425 K, are shown in Fig. 3. As these curves show, increasing stress at a constant temperature results in higher penetration rates. It can further be seen that after a rather short primary creep stage almost all of the curves show a relatively long steady-state region where depth increases linearly with time. Since the impression creep test is compressive in nature, necking and fracture of the specimen do not occur and hence, it is obviously not possible to record a third stage of the curve, as opposed to that which normally happens in an ordinary creep test [13].

Figs. 4a and 4b show comparisons of impression creep curves under the punching stresses of 500 MPa at 425 K and 450 MPa at 455 K, respectively. It can be observed that the introduction of RE and Zr into AZ91 generally improves its creep resistance. The lowest level and slope in the steady state region belong to the AZ91-2RE alloy, the highest to the AZ91 alloy, with the remaining alloys lying between. In other

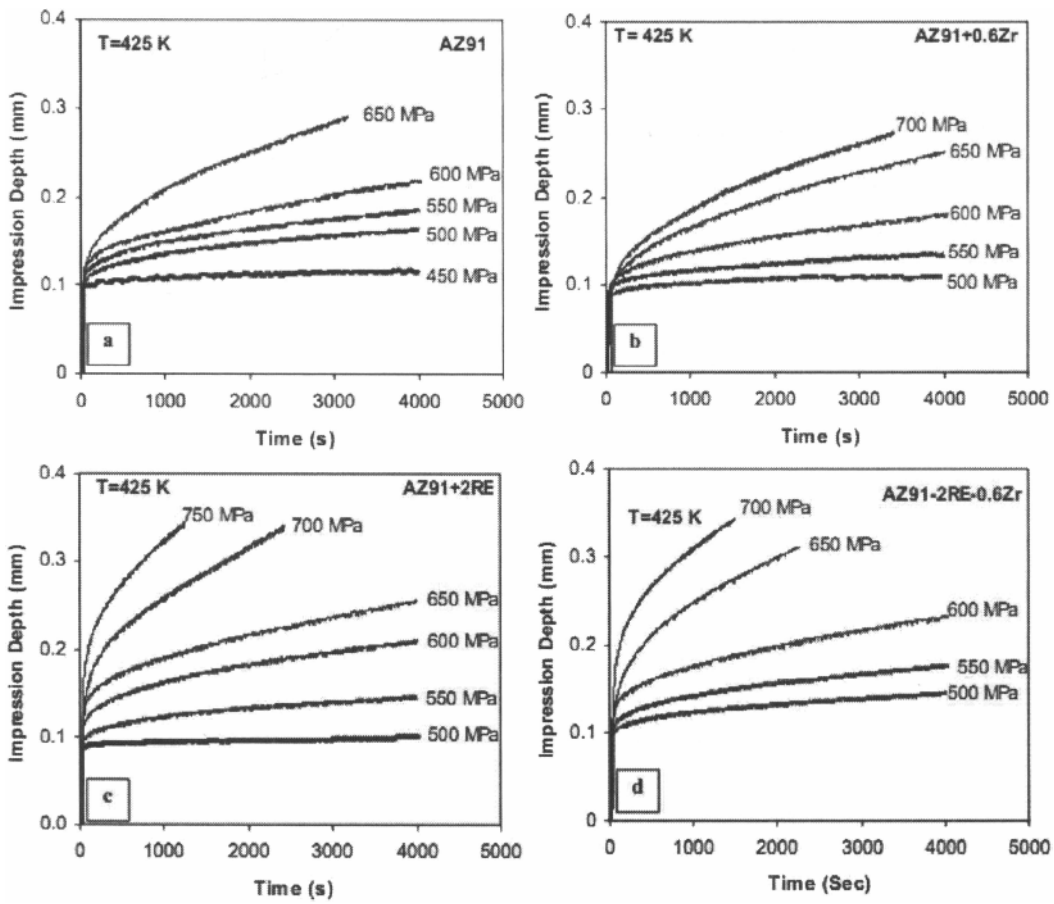

Figure 3. Typical creep curves of the investigated alloys at 425 K under different stress levels: (a) AZ91, (b) AZ91-0.6Zr, (c) AZ91-2RE, and (d) AZ91-2RE-0.6Zr alloy.

words, 2%RE addition has the strongest effect on the creep resistance, followed by 0.6%Zr addition. Simultaneous addition of RE and Zr, however, has the least effect on the enhancement of creep resistance. As shown in Fig. 4, the creep performance of AZ91-2RE-0.6Zr is inferior to that of AZ91-2RE and AZ91-0.6Zr, even though AZ91-2RE-0.6Zr contains both Al-Zr and Al-RE intermetallics. This may emphasize the effect of solid solution hardening as one of the most important strengthening mechanism in AZ91 with high percentage of aluminum content. Since testing temperatures in this investigation are not high enough to accelerate diffusion process through the matrix, it can be concluded that solute aluminum atoms are still playing an important role in the hardening of the material. Formation of higher volumes of Al-containing intermetallics in AZ91-2RE-0.6Zr, compared to both AZ91-2RE and AZ91-0.6Zr, leaves less Al solute atoms through the microstructure of the former alloy. In other words, drop of creepresistance due to the loss of solid solution hardening cannot be compensated by formation of larger volumes of the thermally stable intermetallics through the microstructure of AZ91-2RE-0.6Zr.

Conclusions

Following previous works in which separate addition of Zr and RE to AZ91 caused significant improvement of creep properties, it was expected simultaneous presence of these elements results in greater enhancement. However, the newly developed AZ91-2RE-0.6Zr alloy turned out to have poorer creep properties than the AZ91-2RE and AZ91-0.6Zr alloys. This is interesting when considering that both of the latter alloys had previously shown the highest levels of creep resistance among different RE-containing and Zr-containing AZ91 alloys by taking advantage of simultaneous solid solution hardening and particle hardening. Despite the higher volume fraction of the thermally stable particles distributed in the microstructure of AZ91-2RE-0.6Zr, it seems that its creep performance suffers from lack of enough solid solution hardening.

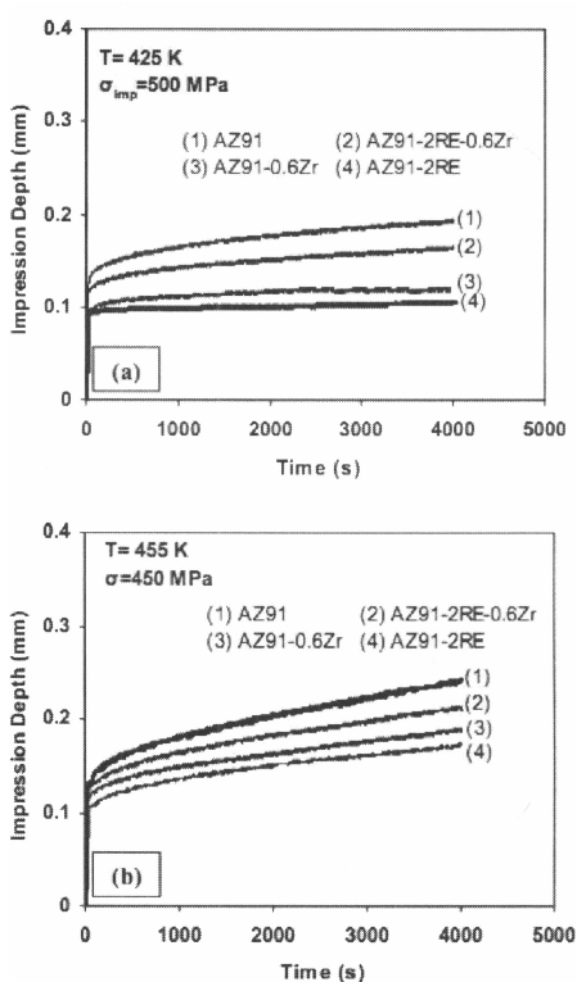

Figure 4. Comparison of creep curves of the investigated alloys at; (a) T = 425 K, σ_{imp} = 500 MPa, and (b) T = 455 K, σ_{imp} =450 MPa.

References

1. I.J. Polmear: Light Alloys, 2nd ed., Chapman and Hall, Inc., New York, NY, 1989, 170.
2. A.A. Luo and M.O. Pekguleryuz, "Cast Magnesium Alloys for Elevated Temperature Applications", Journal of Materials Science, 29 (1994), 5259-71.
3. A.A. Luo, "Recent Magnesium Alloy Development for Elevated Temperature Application", International Materials Review, 49 (2004), 13-30.
4. G.L. Song and A. Atrens, "Corrosion Mechanisms of Magnesium Alloys", Advanced Engineering Materials, 1 (1999), 11-33.
5. G.L. Song and A. Atrens, "Understanding Magnesium Corrosion. A Framework for Improved Alloy Performance", Advanced Engineering Materials, 5 (2003) 837-858.
6. E. Aghion, B. Bronfin, F. Von Buch, S. Shumann and H. Friedrich, "Newly Developed Magnesium Alloys for Powertrain Applications", JOM, 55 (2003), 30-33.
7. B. Kondori and R. Mahmudi, "Impression Creep Characteristics of a Cast Mg Alloy", Metallurgical and Materials Transactions A, 40 (2009) 2007-2015.
8. B. Kondori and R. Mahmudi, "Effect of Ca Additions on the Microstructure, Thermal Stability and Mechanical Properties of a Cast AM60 Magnesium Alloy", Materials Science and Engineering A, 527 (2010) 2014-2021.
9. F. Kabirian and R. Mahmudi, "Effects of Rare Earth Element Additions on the Impression Creep Behavior of AZ91 Magnesium Alloy", Metallurgical and Materials Transactions A, 40 (2009), 2190-2201.
10. F. Kabirian and R. Mahmudi, "Effects of Zr Additions on the Microstructure and Impression Creep Behavior of AZ91 Magnesium Alloy", Metallurgical and Materials Transactions A, 41 (2010), 3488-3498.
11. F. Kabirian and R. Mahmudi, "Effects of Zirconium Additions on the Microstructure of As-Cast and Aged AZ91 Magnesium Alloy", Advanced Engineering Materials, 11 (2009), 189-193.